Structural Engineering and Mechanics, *Vol. 47, No. 3 (2013) 361-381*
DOI: http://dx.doi.org/10.12989/sem.2013.47.3.361

Online estimation of noise parameters for Kalman filter

Ka-Veng Yuen*, Peng-Fei Liang[a] and Sin-Chi Kuok[b]

Department of Civil and Environmental Engineering, Faculty of Science and Technology, University of Macau, Macao, China

(Received April 15, 2013, Revised July 19, 2013, Accepted July 30, 2013)

Abstract. A Bayesian probabilistic method is proposed for online estimation of the process noise and measurement noise parameters for Kalman filter. Kalman filter is a well-known recursive algorithm for state estimation of dynamical systems. In this algorithm, it is required to prescribe the covariance matrices of the process noise and measurement noise. However, inappropriate choice of these covariance matrices substantially deteriorates the performance of the Kalman filter. In this paper, a probabilistic method is proposed for online estimation of the noise parameters which govern the noise covariance matrices. The proposed Bayesian method not only estimates the optimal noise parameters but also quantifies the associated estimation uncertainty in an online manner. By utilizing the estimated noise parameters, reliable state estimation can be accomplished. Moreover, the proposed method does not assume any stationarity condition of the process noise and/or measurement noise. By removing the stationarity constraint, the proposed method enhances the applicability of the state estimation algorithm for nonstationary circumstances generally encountered in practice. To illustrate the efficacy and efficiency of the proposed method, examples using a fifty-story building with different stationarity scenarios of the process noise and measurement noise are presented.

Keywords: Bayesian probabilistic approach; Kalman filter; online algorithm; process noise; measurement noise; structural health monitoring

1. Introduction

Kalman filter is a well-known recursive algorithm for state estimation of dynamical systems (Kalman 1960). Due to its potential for online state estimation, Kalman filter has been extensively applied in various engineering disciplines (Schmidt 1981, Grewal and Andrews 1993, Hoi *et al*. 2008, Chui and Chen 2009, Lee and Chen 2010, Lei and Jiang 2011, Papadimitriou *et al*. 2011, Lin *et al*. 2013). Despite its wide range of applications, this algorithm requires to prescribe the covariance matrices of the process noise and measurement noise. The accuracy of state estimation depends on the prior selection of these covariance matrices and inappropriate choice substantially deteriorates its performance. Since reliable prior information of the time-varying noise covariance matrices is generally not available in practice, the reliability of the state estimation is questionable

*Corresponding author, Professor, E-mail: kvyuen@umac.mo
[a]Master Student, E-mail: liangpengfei211@gmail.com
[b]Ph.D. Candidate, E-mail: sckuok@gmail.com

http://www.techno-press.org/?journal=sem&subpage=8 ISSN: 1225-4568 (Print), 1598-6217 (Online)

(Sangsuk-Iam and Bullock 1990).

To address this issue, a number of methods have been proposed to estimate the noise covariance matrices. Mehra (1970) proposed to optimize the Kalman gain matrix and the noise covariance matrices by using the autocorrelation function of the residuals between the measurement and the corresponding estimated state. Koh and See (1994) introduced a covariance matching technique to update the noise parameters. With a moving time window prescribed by the user, the noise parameters are updated according to the predicted state trajectories of batches of past data. Mohamed and Schwarz (1999) presented a maximum likelihood method to determine the optimal noise parameters by maximizing the likelihood function of the measurements. Odelson *et al*. (2006) proposed an autocovariance least-squares method to estimate the noise covariance matrices. The autocovariance of the residuals of the output states is utilized so that the optimization problem is converted to a standard least-squares problem. Yuen *et al*. (2007) developed an offline probabilistic approach to estimate the noise parameters. The optimal noise parameters are obtained by maximizing its likelihood function. A half-or-double optimization scheme was proposed to efficiently obtain the estimated noise parameters with acceptable precision. Unfortunately, most of the existing methods are operated in an offline or quasi-online manner.

In this paper, a Bayesian probabilistic method is proposed for online estimation of the noise parameters. Bayesian inference provides a rigorous framework for parametric identification and uncertainty quantification (Box and Tiao 1973, Beck 2010, Yuen and Kuok 2011). It has been developed and applied to various problems in civil engineering (Beck and Katafygiotis 1998, Papadimitriou *et al*. 2000, Beck and Yuen 2004, Yuen and Katafygiotis 2005a, Yuen and Katafygiotis 2005b, Ching *et al*. 2006, Lam *et al*. 2006, Ching *et al*. 2009, Yan *et al*. 2009, Yuen and Kuok 2010, Kuok and Yuen 2012, Yuen and Mu 2012). Taking the advantage of Bayesian inference, the proposed method provides not only the optimal estimation of the noise parameters but also the associated estimation uncertainty. In contrast to most of the works in the literature, the proposed method propagates simultaneously with the state estimation of the Kalman filter algorithm. In other words, the noise parameters are updated for every time step in an online manner.

The crux of the proposed method is given as follows. By utilizing the estimation of the previous time step and the measurement at the current time step, the posterior probability density function (PDF) of the noise parameters is formulated. Then, the optimal noise parameters can be estimated by maximizing the posterior PDF. Meanwhile, the estimation uncertainty of the noise parameters is quantified in terms of the covariance matrix. Thereafter, the estimated noise parameters and the associated covariance matrix will be used to construct the prior distribution for the next time step. The major difficulty of this problem is to efficiently solve the optimization problem especially at the early propagation stage in which the parameter uncertainty is large. By employing the proposed algorithm along with the propagation of the Kalman filter algorithm, online estimation of the noise parameters and the associated covariance matrix can be obtained. Based on the reliable estimation of the noise parameters, accurate state estimation can be accomplished. Since no iteration is required in the algorithm, the proposed method is computationally efficient. Moreover, the proposed method enhances the applicability of the Kalman filter since it does not require any stationarity condition of the process noise and measurement noise. In the conventional usage of Kalman filter, the covariance matrices of the process noise and measurement noise are prescribed constant matrices. This implies the stationarity assumption of the noise processes but this is usually not fulfilled in practice (Yun *et al*.

1979, Yang *et al*. 2004, Taranath 2005, Ni *et al*. 2007, Rosa *et al*. 2012). By removing the stationarity requirement in the proposed method, the applicability of the Kalman filter is substantially widen for nonstationary circumstances.

This paper is organized as follows. In Section 2, the formulation and fundamentals of Kalman filter are briefly reviewed. In Section 3, the proposed Bayesian probabilistic method is presented for online estimation of the noise parameters. This computationally efficient method is a two-stage approach. A training stage is necessary at the early propagation stage while the gradient method is used in the operating stage after the training stage. Thereafter, the procedure of the proposed algorithm is summarized in Section 3.3. Finally, in Section 4, the proposed method is demonstrated with a fifty-story building under different stationarity scenarios of the process noise and measurement noise.

2. Formulation and Kalman filter

Consider a second-order linear dynamical system with N_d degrees of freedom (DOFs) and its equation of motion is given by

$$\mathbf{M}\ddot{\mathbf{x}}(t) + \mathbf{L}\dot{\mathbf{x}}(t) + \mathbf{K}\mathbf{x}(t) = \mathbf{T}_0\mathbf{f}(t) \tag{1}$$

where $\mathbf{x}$ is the generalized displacement vector of the system; $\mathbf{M}$, $\mathbf{L}$ and $\mathbf{K}$ are the mass, damping and stiffness matrix of the system, respectively; $\mathbf{T}_0 \in \mathbb{R}^{N_d \times N_f}$ is the force distributing matrix and $\mathbf{f}(t) \in \mathbb{R}^{N_f}$ is the excitation subjected to the system. The external excitation (i.e., the process noise) $\mathbf{f}$ consists of the deterministic and stochastic components

$$\mathbf{f}(t) = \mathbf{F}_D(t) + \mathbf{F}(t) \tag{2}$$

where $\mathbf{F}_D(t)$ is the deterministic component, and $\mathbf{F}(t)$ is the stochastic component, modeled as a Gaussian process with zero mean and covariance matrix $\mathbf{\Sigma}_f(t)$. Therefore, the external excitation $\mathbf{f}$ is a Gaussian process with mean $\mathbf{F}_D(t)$ and covariance matrix $\mathbf{\Sigma}_f(t)$.

The state vector $\mathbf{y}$ is defined to include the displacement and velocity vector

$$\mathbf{y}(t) \equiv [\mathbf{x}(t)^T, \dot{\mathbf{x}}(t)^T]^T \tag{3}$$

Then, Eq. (1) can be transformed to the state-space form

$$\dot{\mathbf{y}}(t) = \mathbf{A}\mathbf{y}(t) + \mathbf{B}\mathbf{f}(t) \tag{4}$$

where the state matrix $\mathbf{A}$ and input distributing matrix $\mathbf{B}$ are given by:

$$\mathbf{A} = \begin{bmatrix} \mathbf{0} & \mathbf{I} \\ -\mathbf{M}^{-1}\mathbf{K} & -\mathbf{M}^{-1}\mathbf{L} \end{bmatrix}$$
$$\mathbf{B} = \begin{bmatrix} \mathbf{0} \\ \mathbf{M}^{-1}\mathbf{T}_0 \end{bmatrix} \tag{5}$$

where $\mathbf{I}$ is the identity matrix. Eq. (4) can be discretized to a difference equation by assuming that the excitation is constant within any time interval, i.e., $\mathbf{f}(k\Delta t + \tau) = \mathbf{f}(k\Delta t), \forall \tau \in [0, \Delta t), k = 0,1,2, \ldots$

$$\mathbf{y}_{k+1} = \mathbf{A}_d\mathbf{y}_k + \mathbf{B}_d\mathbf{f}_k \tag{6}$$

where $\mathbf{A}_d = \exp(\mathbf{A}\Delta t)$, $\mathbf{B}_d = \mathbf{A}^{-1}(\mathbf{A}_d - \mathbf{I})\mathbf{B}$, $\mathbf{f}_k = \mathbf{F}_{D,k} + \mathbf{F}_k$, Δt is the sampling time step, $\mathbf{y}_k \equiv \mathbf{y}(k\Delta t)$, $\mathbf{f}_k \equiv \mathbf{f}(k\Delta t)$, $\mathbf{F}_{D,k} \equiv \mathbf{F}_D(k\Delta t)$ and $\mathbf{F}_k \equiv \mathbf{F}(k\Delta t)$. The discrete external excitation $\mathbf{f}_k$ is a discrete Gaussian process with mean $\mathbf{F}_{D,k}$ and covariance matrix $\boldsymbol{\Sigma}_{f,k}(\boldsymbol{\theta}_{f,k})$, where $\boldsymbol{\theta}_{f,k}$ is the characteristic parameter vector of the covariance matrix $\boldsymbol{\Sigma}_{f,k}$.

Discrete-time response measurement is available at N_0 observed DOFs and this noise corrupted output measurement is modeled as

$$\mathbf{z}_{k+1} = \mathbf{C}_d\mathbf{y}_{k+1} + \mathbf{D}_d\mathbf{F}_{D,k+1} + \mathbf{n}_{k+1} \tag{7}$$

where $\mathbf{C}_d \in \mathbb{R}^{N_0 \times 2N_d}$ is the observation matrix; and $\mathbf{D}_d \in \mathbb{R}^{N_0 \times N_f}$ is the input distributing matrix of the deterministic excitation component to the output. Given a sensor configuration, these matrices can be easily obtained. The measurement noise $\mathbf{n}$ is modeled as an N_0-variate discrete Gaussian process with zero mean and covariance matrix $\boldsymbol{\Sigma}_{n,k+1}(\boldsymbol{\theta}_{n,k+1})$ at the kth time step, where $\boldsymbol{\theta}_{n,k+1}$ is the characteristic parameter vector of the covariance matrix $\boldsymbol{\Sigma}_{n,k+1}$. Furthermore, it is assumed that the measurement noise $\mathbf{n}$ and the process noise $\mathbf{f}$ are statistically independent.

The essential steps of the Kalman filter algorithm are to predict and filter/update in an alternating manner at each time step using the available data set. Given the measurements up to the kth time step $D_k = \{\mathbf{z}_1, \mathbf{z}_2, \ldots, \mathbf{z}_k\}$, the state vector $\mathbf{y}_{k+1}$ can be predicted by using its conditional probability density function (PDF) $p(\mathbf{y}_{k+1}|D_k)$, which follows a multi-variate Gaussian distribution. By using Eq. (6), the one-step-ahead predicted state vector at the $(k+1)$th time step can be obtained

$$\mathbf{e}_{y,k+1} \equiv E[\mathbf{y}_{k+1}|D_k] = \mathbf{A}_d\bar{\mathbf{e}}_{y,k} + \mathbf{B}_d\mathbf{F}_{D,k} \tag{8}$$

where $\bar{\mathbf{e}}_{y,k} \equiv E[\mathbf{y}_k|D_k]$ is the filtered state of the previous time step. In addition, the uncertainty of the predicted state can be represented by its covariance matrix

$$\boldsymbol{\Sigma}_{y,k+1} \equiv E\left[(\mathbf{y}_{k+1} - \mathbf{e}_{y,k+1})(\mathbf{y}_{k+1} - \mathbf{e}_{y,k+1})^T \middle| D_k\right] = \mathbf{A}_d\bar{\boldsymbol{\Sigma}}_{y,k}\mathbf{A}_d^T + \mathbf{B}_d\boldsymbol{\Sigma}_{f,k}\mathbf{B}_d^T \tag{9}$$

where $\bar{\boldsymbol{\Sigma}}_{y,k} \equiv E\left[(\mathbf{y}_k - \bar{\mathbf{e}}_{y,k})(\mathbf{y}_k - \bar{\mathbf{e}}_{y,k})^T \middle| D_k\right]$ represents the filtered/updated state covariance matrix at the kth time step using the measurements up to the same time step. When the measurement at the $(k+1)$th time step is available, the updated state vector $\bar{\mathbf{e}}_{y,k+1}$ can be obtained by maximizing the conditional PDF $p(\mathbf{y}_{k+1}|D_{k+1})$

$$\bar{\mathbf{e}}_{y,k+1} = \mathbf{e}_{y,k+1} + \mathbf{K}_{k+1}(\mathbf{z}_{k+1} - \mathbf{C}_d\mathbf{e}_{y,k+1} - \mathbf{D}_d\mathbf{F}_{D,k+1}) \tag{10}$$

where the Kalman gain $\mathbf{K}_{k+1}$ is given by (Kalman 1960)

$$\mathbf{K}_{k+1} = \boldsymbol{\Sigma}_{y,k+1}\mathbf{C}_d^T(\mathbf{C}_d\boldsymbol{\Sigma}_{y,k+1}\mathbf{C}_d^T + \boldsymbol{\Sigma}_{n,k+1})^{-1} \tag{11}$$

Again, the uncertainty of the updated state vector is represented by its covariance matrix

$$\bar{\boldsymbol{\Sigma}}_{y,k+1} = (\mathbf{I} - \mathbf{K}_{k+1}\mathbf{C}_d)\boldsymbol{\Sigma}_{y,k+1} \tag{12}$$

Eqs. (8), (9), (10) and (12) comprise the essential propagation formulae of the Kalman filter algorithm (Kalman 1960, Grewal and Andrews 1993). It is obvious that the accuracy of the estimated state vectors and their covariance matrices depends on the process noise and measurement noise parameters which are unknown in practice. In the following section, the proposed Bayesian probabilistic approach is presented for online estimation of these noise parameters.

3. Online estimation of the noise parameters

3.1 Bayesian probabilistic approach

The covariance matrices of the process noise and measurement noise are parameterized as: $\boldsymbol{\Sigma}_{f,k} = \boldsymbol{\Sigma}_{f,k}(\boldsymbol{\theta}_{f,k})$ and $\boldsymbol{\Sigma}_{n,k+1} = \boldsymbol{\Sigma}_{n,k+1}(\boldsymbol{\theta}_{n,k+1})$. Then, the noise parameter vector to be estimated at the $(k+1)$th time step $\boldsymbol{\theta}_{k+1} \in \mathbb{R}^{N_\theta}$ can be defined to include the process noise parameter vector $\boldsymbol{\theta}_{f,k}$ and the measurement noise parameter vector $\boldsymbol{\theta}_{n,k+1}$

$$\boldsymbol{\theta}_{k+1} = \left[\boldsymbol{\theta}_{f,k}^T, \boldsymbol{\theta}_{n,k+1}^T\right]^T \tag{13}$$

The primary objective of this research is to develop an efficient algorithm for online estimation of these noise parameters. By using the Bayes' theorem, the posterior PDF of the noise parameter vector $\boldsymbol{\theta}_{k+1}$ given the measurement data set D_{k+1} is (Yuen and Katafygiotis 2001)

$$p(\boldsymbol{\theta}_{k+1}|\mathbf{z}_{k+1}, D_k) = c_0 p(\boldsymbol{\theta}_{k+1}|D_k) p(\mathbf{z}_{k+1}|\boldsymbol{\theta}_{k+1}, D_k) \tag{14}$$

where $p(\boldsymbol{\theta}_{k+1}|D_k)$ is the prior PDF; $p(\mathbf{z}_{k+1}|\boldsymbol{\theta}_{k+1}, D_k)$ is the likelihood function; and c_0 is the normalizing constant such that integrating the right-hand side over the entire domain of $\boldsymbol{\theta}_{k+1}$ yields unity. The prior distribution $p(\boldsymbol{\theta}_{k+1}|D_k)$ is approximated as a Gaussian distribution. By considering certain continuity of the noise parameters, the mean is taken as the estimation from the previous time step $\bar{\mathbf{e}}_{\theta,k}$ and the covariance matrix is $\lambda\overline{\boldsymbol{\Sigma}}_{\theta,k}$, where $\bar{\mathbf{e}}_{\theta,k}$ and $\overline{\boldsymbol{\Sigma}}_{\theta,k}$ are the updated noise parameter vector and the associated covariance matrix of the previous time step. The fading factor $\lambda \geq 1$ is assigned to enlarge the estimated covariance matrix so that the contribution of the past data is discounted gradually (Sorensen and Sacks 1971, Grewal and Andrews 1993). Here, it is used to activate the adaptiveness of the proposed algorithm in order to track the time-varying noise parameters. In the special case when a unity fading factor (i.e., $\lambda = 1$) is employed, there is no discounting effect on the past data. In this study, the fading factor is chosen as $\lambda = 2^{2/N_s}$ so that the half-life of the contribution of a data point is N_s time steps. As a result, the prior distribution can be expressed as follows

$$p(\boldsymbol{\theta}_{k+1}|D_k) = (2\pi)^{-\frac{N_\theta}{2}} \left|\lambda\overline{\boldsymbol{\Sigma}}_{\theta,k}\right|^{-\frac{1}{2}} \exp\left[-\frac{1}{2\lambda}\left(\boldsymbol{\theta}_{k+1} - \bar{\mathbf{e}}_{\theta,k}\right)^T \overline{\boldsymbol{\Sigma}}_{\theta,k}^{-1}\left(\boldsymbol{\theta}_{k+1} - \bar{\mathbf{e}}_{\theta,k}\right)\right] \tag{15}$$

The usage of this prior distribution can be viewed as a regularizer. It facilitates the identifiability of the optimization problem even when there are unnecessarily too many noise parameters. However, it affects the computational cost of the proposed algorithm. In practical circumstances, it is suggested to use no more than five noise parameters to avoid overfitting. In this case, the computational cost of the proposed method is acceptable.

The likelihood function $p(\mathbf{z}_{k+1}|\boldsymbol{\theta}_{k+1}, D_k)$ reflects the contribution of the measurement $\mathbf{z}_{k+1}$ in establishing the posterior PDF of the noise parameters and it is given by

$$p(\mathbf{z}_{k+1}|\boldsymbol{\theta}_{k+1}, D_k) = (2\pi)^{-\frac{N_0}{2}} \left|\boldsymbol{\Sigma}_{z,k+1}\right|^{-\frac{1}{2}} \exp\left[-\frac{1}{2}\left(\mathbf{z}_{k+1} - \mathbf{e}_{z,k+1}\right)^T \boldsymbol{\Sigma}_{z,k+1}^{-1}\left(\mathbf{z}_{k+1} - \mathbf{e}_{z,k+1}\right)\right] \tag{16}$$

where the estimator $\mathbf{e}_{z,k+1}$ can be obtained by taking the expectation of Eq. (7)

$$\mathbf{e}_{z,k+1} \equiv E[\mathbf{z}_{k+1}|D_k] = \mathbf{C}_d \mathbf{e}_{y,k+1} + \mathbf{D}_d \mathbf{F}_{D,k+1} \tag{17}$$

Based on Eqs. (7), (9) and (17), the associated covariance matrix $\boldsymbol{\Sigma}_{z,k+1}$ can be readily obtained

$$\begin{aligned}\boldsymbol{\Sigma}_{z,k+1} &\equiv E\left[\left(\mathbf{z}_{k+1}-\mathbf{e}_{z,k+1}\right)\left(\mathbf{z}_{k+1}-\mathbf{e}_{z,k+1}\right)^T\middle| D_k\right] \\ &= \mathbf{C}_d\mathbf{A}_d\overline{\boldsymbol{\Sigma}}_{y,k}\mathbf{A}_d^T\mathbf{C}_d^T + \mathbf{C}_d\mathbf{B}_d\boldsymbol{\Sigma}_{f,k}\mathbf{B}_d^T\mathbf{C}_d^T + \boldsymbol{\Sigma}_{n,k+1}\end{aligned} \tag{18}$$

Note that the noise parameters appear implicitly on the right hand side of Eq. (16) through $\boldsymbol{\Sigma}_{z,k+1}$.

By substituting Eqs. (15) and (16) into Eq. (14), the posterior PDF $p(\boldsymbol{\theta}_{k+1}|D_{k+1})$ can be rewritten as follows

$$\begin{aligned}p(\boldsymbol{\theta}_{k+1}|D_{k+1}) = c_1\left|\boldsymbol{\Sigma}_{z,k+1}\right|^{-\frac{1}{2}}\exp\Bigg[&-\frac{1}{2\lambda}\left(\boldsymbol{\theta}_{k+1}-\bar{\mathbf{e}}_{\theta,k}\right)^T\overline{\boldsymbol{\Sigma}}_{\theta,k}^{-1}\left(\boldsymbol{\theta}_{k+1}-\bar{\mathbf{e}}_{\theta,k}\right) \\ &-\frac{1}{2}\left(\mathbf{z}_{k+1}-\mathbf{e}_{z,k+1}\right)^T\boldsymbol{\Sigma}_{z,k+1}^{-1}\left(\mathbf{z}_{k+1}-\mathbf{e}_{z,k+1}\right)\Bigg]\end{aligned} \tag{19}$$

where the constant $c_1 = c_0(2\pi)^{-\frac{(N_O+N_\theta)}{2}}\left|\lambda\overline{\boldsymbol{\Sigma}}_{\theta,k}\right|^{-\frac{1}{2}}$ does not depend on the noise parameters in $\boldsymbol{\theta}_{k+1}$.

Then, the objective function $J(\boldsymbol{\theta}_{k+1})$ can be defined as the negative logarithm of the posterior PDF $p(\boldsymbol{\theta}_{k+1}|D_{k+1})$ without including the constant term

$$\begin{aligned}J(\boldsymbol{\theta}_{k+1}) = \frac{1}{2}\Bigg[&\ln\left|\boldsymbol{\Sigma}_{z,k+1}\right| + \frac{1}{\lambda}\left(\boldsymbol{\theta}_{k+1}-\bar{\mathbf{e}}_{\theta,k}\right)^T\overline{\boldsymbol{\Sigma}}_{\theta,k}^{-1}\left(\boldsymbol{\theta}_{k+1}-\bar{\mathbf{e}}_{\theta,k}\right) \\ &+\left(\mathbf{z}_{k+1}-\mathbf{e}_{z,k+1}\right)^T\boldsymbol{\Sigma}_{z,k+1}^{-1}\left(\mathbf{z}_{k+1}-\mathbf{e}_{z,k+1}\right)\Bigg]\end{aligned} \tag{20}$$

Therefore, the updated noise parameter vector $\bar{\mathbf{e}}_{\theta,k+1}$ can be obtained by maximizing the posterior PDF $p(\boldsymbol{\theta}_{k+1}|D_{k+1})$ or, equivalently, by minimizing the objective function $J(\boldsymbol{\theta}_{k+1})$

$$\bar{\mathbf{e}}_{\theta,k+1} = \arg\min_{\boldsymbol{\theta}_{k+1}} J(\boldsymbol{\theta}_{k+1}) \tag{21}$$

Since there is no closed-form solution for this optimization problem, a computationally efficient procedure is proposed to obtain the numerical solution and the details will be presented in Section 3.2.

Furthermore, the associated uncertainty of the estimation is represented by the covariance matrix $\overline{\boldsymbol{\Sigma}}_{\theta,k+1}$ which can be calculated by

$$\overline{\boldsymbol{\Sigma}}_{\theta,k+1} = \left[\boldsymbol{H}_J\left(\bar{\mathbf{e}}_{\theta,k+1}\right)\right]^{-1} \tag{22}$$

where $\boldsymbol{H}_J\left(\bar{\mathbf{e}}_{\theta,k+1}\right)$ is the Hessian matrix of the objective function evaluated at $\boldsymbol{\theta}_{k+1} = \bar{\mathbf{e}}_{\theta,k+1}$ and it can be computed efficiently using the finite difference method. Specifically, its (l, l') component is given by Yuen (2010)

$$\begin{aligned}\boldsymbol{H}_J^{(l,l')}\left(\bar{\mathbf{e}}_{\theta,k+1}\right) &\equiv \left.\frac{\partial^2 J(\boldsymbol{\theta}_{k+1})}{\partial\theta_{k+1}^{(l)}\partial\theta_{k+1}^{(l')}}\right|_{\boldsymbol{\theta}_{k+1}=\bar{\mathbf{e}}_{\theta,k+1}} \\ &= \begin{cases}\left(\frac{1}{\Delta\theta^{(l)}}\right)^2\left[J\left(\bar{\mathbf{e}}_{\theta,k+1}+\Delta\boldsymbol{\theta}_l\right)-2J\left(\bar{\mathbf{e}}_{\theta,k+1}\right)+J\left(\bar{\mathbf{e}}_{\theta,k+1}-\Delta\boldsymbol{\theta}_l\right)\right], l=l' \\ \frac{1}{4\Delta\theta^{(l)}\Delta\theta^{(l')}}\left[J\left(\bar{\mathbf{e}}_{\theta,k+1}+\Delta\boldsymbol{\theta}_l+\Delta\boldsymbol{\theta}_{l'}\right)-J\left(\bar{\mathbf{e}}_{\theta,k+1}-\Delta\boldsymbol{\theta}_l+\Delta\boldsymbol{\theta}_{l'}\right)-J\left(\bar{\mathbf{e}}_{\theta,k+1}+\Delta\boldsymbol{\theta}_l-\Delta\boldsymbol{\theta}_{l'}\right)+J\left(\bar{\mathbf{e}}_{\theta,k+1}-\Delta\boldsymbol{\theta}_l-\Delta\boldsymbol{\theta}_{l'}\right)\right], l\neq l'\end{cases}\end{aligned} \tag{23}$$

where the perturbation vectors $\Delta\theta_l = [0, \ldots, 0, \Delta\theta^{(l)}, 0, \ldots, 0]^T$ and $\Delta\theta_{l'} = [0, \ldots, 0, \Delta\theta^{(l')}, 0, \ldots, 0]^T$

are vectors with zero entries except the *l*th and *l*'th components being small positive perturbations $\Delta\theta^{(l)}$ and $\Delta\theta^{(l')}$, respectively. At the early propagation stage, the updated covariance matrix of the noise parameter vector $\overline{\boldsymbol{\Sigma}}_{\theta,k+1}$ may not satisfy the positive-definiteness condition of covariance matrices since the approximation in Eq. (22) is inaccurate. In this situation, the updated covariance matrix $\overline{\boldsymbol{\Sigma}}_{\theta,k+1}$ will be replaced by the covariance matrix of the previous time step $\overline{\boldsymbol{\Sigma}}_{\theta,k}$.

From Eqs. (20) to (22), it can be seen that the computation cost of the proposed algorithm depends on $\overline{\boldsymbol{\Sigma}}_{\theta,k}$ and $\boldsymbol{\Sigma}_{z,k+1}$. The size of $\overline{\boldsymbol{\Sigma}}_{\theta,k}$ is $N_\theta \times N_\theta$ and it depends on the number of noise parameters of the noise covariance matrices, N_θ. In general, this number is much smaller than the number of degrees of freedom, N_d. On the other hand, the size of $\boldsymbol{\Sigma}_{z,k+1}$ is $N_0 \times N_0$, where the number of measured degrees of freedom, N_0, is again much smaller than N_d. Therefore, the addition computation cost of the proposed algorithm is very minor, compared with the Kalman filter algorithm itself. In the following, a computationally efficient algorithm is proposed to solve Eq. (21) so that the noise parameters can be estimated in an online manner.

3.2 Proposed optimization algorithm

In this section, an efficient two-stage algorithm is proposed for the optimization problem in Eq. (21) in order to estimate the noise parameters in an online manner. This algorithm consists of the training stage and the operating stage. Specifically, the optimization problem is solved using an online half-or-double optimization algorithm during the training stage while it is solved using the gradient method during the operating stage.

3.2.1 Training stage

At the early propagation stage, the posterior PDF is associated with large uncertainty and complicated topology since only a limited number of data points have been acquired. Furthermore, the initial values of the noise parameters may be far away from the actual values. Therefore, direct application of gradient-type of methods at this stage may lead to erroneous results. This is the major reason in hampering the development of an efficient online identification method for the noise parameters. In order to overcome this difficulty, a training process is introduced at the early propagation stage. In this stage, an online half-or-double optimization algorithm is utilized. First, the parameter candidate set is established based on the half-or-double rule of the solution from the previous time step and it is given by

$$\boldsymbol{\Theta} = \left\{ \boldsymbol{\theta}_{k+1} : \theta_{k+1}^{(l)} = \varphi_l \bar{\mathrm{e}}_{\theta,k}^{(l)};\ \varphi_l = 1/2, 1, 2 \right\} \tag{24}$$

where $\bar{\mathrm{e}}_{\theta,k}^{(l)}$ is the lth component of the updated noise parameter vector at the kth time step $\bar{\mathbf{e}}_{\theta,k}$. The optimal solution for the (k+1)th time step is the parameter vector candidate which provides the minimum objective function value within the parameter candidate set $\boldsymbol{\Theta}$

$$\bar{\mathbf{e}}_{\theta,k+1} = \arg \min_{\boldsymbol{\theta}_{k+1} \in \boldsymbol{\Theta}} J(\boldsymbol{\theta}_{k+1}) \tag{25}$$

The training stage will be terminated if the training has been carried out for no less than one fundamental period of the concerned dynamical system and the updated noise parameter vectors are identical for ten consecutive time steps.

3.2.2 Operating stage

At the end of the training stage, a preliminary solution (which is relatively close to the true optimal point of the posterior PDF) of the noise parameters has been obtained. Furthermore, since the topology of the posterior PDF will become more regular at this stage after acquiring a considerable amount of data points, it is possible to use the gradient method to solve the optimization problem. Specifically, the updated noise parameter vector can be obtained as follows

$$\bar{\mathbf{e}}_{\theta,k+1} = \bar{\mathbf{e}}_{\theta,k} - \bar{\boldsymbol{\Sigma}}_{\theta,k} \nabla J\left(\bar{\mathbf{e}}_{\theta,k}\right) \tag{26}$$

where the matrix $\bar{\boldsymbol{\Sigma}}_{\theta,k}$ is given by Eq. (22) (with $k+1$ being replaced by k); and $\nabla J\left(\bar{\mathbf{e}}_{\theta,k}\right)$ is the gradient of the objective function evaluated at $\boldsymbol{\theta}_k = \bar{\mathbf{e}}_{\theta,k}$. It can be computed numerically using the finite difference method and its lth component is given by

$$\nabla J^{(l)}\left(\bar{\mathbf{e}}_{\theta,k}\right) \equiv \left.\frac{\partial J(\boldsymbol{\theta}_{\mathrm{k}})}{\partial \theta_k^{(l)}}\right|_{\boldsymbol{\theta}_k = \bar{\mathbf{e}}_{\theta,k}} = \frac{1}{2\Delta\theta^{(l)}}\left[J\left(\bar{\mathbf{e}}_{\theta,k} + \Delta\boldsymbol{\theta}_l\right) - J\left(\bar{\mathbf{e}}_{\theta,k} - \Delta\boldsymbol{\theta}_l\right)\right] \tag{27}$$

where $\Delta\boldsymbol{\theta}_l = \left[0, \ldots, 0, \Delta\theta^{(l)}, 0, \ldots, 0\right]^T$. It is worth noting that the contribution of one data point is small. Therefore, the estimated noise parameter vectors in two consecutive time steps are expected to be close to each other. Consequently, Eq. (26) provides accurate solution for the optimization problem without any iteration.

3.3 Summary of the proposed method

The proposed method can be summarized as follows:

Training stage

1. Initialize arbitrarily (subjected to positive or positive-definite condition) the state vector $\bar{\mathbf{e}}_{y,0}$, noise parameter vector $\bar{\mathbf{e}}_{\theta,0}$ and covariance matrices $\bar{\boldsymbol{\Sigma}}_{y,0}$ and $\bar{\boldsymbol{\Sigma}}_{\theta,0}$.

2. Calculate the predicted state vector $\mathbf{e}_{y,k+1}$ and the associated covariance matrix $\boldsymbol{\Sigma}_{y,k+1}$ by using Eqs. (8) and (9), respectively.

3. Estimate the updated noise parameter vector $\bar{\mathbf{e}}_{\theta,k+1}$ according to Eqs. (24) and (25).

4. Compute the covariance matrix of the updated noise parameter vector $\bar{\boldsymbol{\Sigma}}_{\theta,k+1}$ by using Eq. (22). If $\bar{\boldsymbol{\Sigma}}_{\theta,k+1}$ does not satisfy the positive-definiteness criterion, replace it by $\bar{\boldsymbol{\Sigma}}_{\theta,k}$.

5. Calculate the updated state vector $\bar{\mathbf{e}}_{y,k+1}$ and the associated covariance matrix $\bar{\boldsymbol{\Sigma}}_{y,k+1}$ by using Eqs. (10) and (12), respectively.

6. Check whether the stopping criteria are satisfied:

a) The training stage has been carried out for at least one fundamental period of the system;

b) The optimal noise parameters remain unchanged for ten consecutive time steps.

If yes, then go to the operating stage. Otherwise, repeat the procedure from Step 2 for the next time step.

Operating stage

7. Calculate the predicted state vector $\mathbf{e}_{y,k+1}$ and the associated covariance matrix $\boldsymbol{\Sigma}_{y,k+1}$ by using Eqs. (8) and (9), respectively.

8. Estimate the updated noise parameter vector $\bar{\mathbf{e}}_{\theta,k+1}$ by using Eq. (26).

9. Compute the covariance matrix of the updated noise parameter vector $\bar{\mathbf{\Sigma}}_{\theta,k+1}$ by using Eq. (22).

10. Calculate the updated state vector $\bar{\mathbf{e}}_{y,k+1}$ and the associated covariance matrix $\bar{\mathbf{\Sigma}}_{y,k+1}$ by using Eqs. (10) and (12), respectively.

11. Repeat the procedure from Step 7 for the next time step.

4. Illustrative example

A fifty-story shear building is utilized to demonstrate the efficacy and applicability of the proposed method. The building has a square floor plan with 20m width and identical interstory height of 2.5m. It is assumed that the building has a uniformly distributed floor mass and interstory stiffness over its height. The floor mass and the interstory stiffness are taken to be 400 metric ton and 652.9MN/m, respectively. As a result, the fundamental frequency of the building is 0.2Hz. Rayleigh damping is assumed, i.e., the damping matrix is given by $\mathbf{L} = \alpha_M \mathbf{M} + \alpha_K \mathbf{K}$, where $\alpha_M = 1.885 \times 10^{-2}\text{s}^{-1}$ and $\alpha_K = 3.980 \times 10^{-3}\text{s}$, so that the damping ratios of the first two modes are 1.00%. Acceleration responses are measured at the 1st, 10th, 20th, 30th, 40th and 50th floor. The entire monitoring duration is 1000s and the sampling frequency is 100Hz. Moreover, the fading factor is taken to be $\lambda = 2^{2/1000} = 1.001387$, implying that the data half-life is 10s.

Three stationarity scenarios of the process noise and measurement noise are considered:

Case 1. stationary ground excitation with stationary measurement noise

Case 2. nonstationary ground excitation with stationary measurement noise

Case 3. nonstationary wind excitation with nonstationary measurement noise

4.1 Case 1: Stationary ground excitation with stationary measurement noise

In Case 1, the underlying shear building is subjected to stationary ground excitation. The force distributing matrix is given by $\mathbf{T}_0 = \mathbf{M}[-1, -1, \ldots, -1]^T$ and the ground excitation is given by $\mathbf{f}(t) = \mathbf{F}(t) = \ddot{g}(t)$. The base acceleration $\ddot{g}$ is modeled as zero-mean stationary Gaussian white noise with spectral intensity $S_{\ddot{g}0} = 1.20 \times 10^{-4}\text{m}^2/\text{s}^3$. The covariance matrix of the excitation can be expressed as $\mathbf{\Sigma}_{f,k} = \sigma_{\ddot{g},k}^2$. On the other hand, the measurement noise is also modeled as zero-mean stationary Gaussian white noise. The root-mean-square (RMS) of the measurement noise is taken to be 5% RMS of the noise-free acceleration of the top floor. Therefore, the covariance matrix of the measurement noise can be expressed as $\mathbf{\Sigma}_{n,k+1} = \sigma_{n,k+1}^2 \mathbf{I}$. The noise parameter vector is assumed to consist of two parameters and it is denoted by $\boldsymbol{\theta}_{k+1} = \left[\theta_{f,k}, \theta_{n,k+1}\right]^T$, where $\theta_{f,k} = \sigma_{\ddot{g},k}^2$ and $\theta_{n,k+1} = \sigma_{n,k+1}^2$. The actual noise parameter vector is $\widehat{\boldsymbol{\theta}} = [0.0754, 1.320 \times 10^{-4}]^T$ and it remains constant throughout the entire estimation process in this case.

The proposed method requires only arbitrary initial noise parameters $\bar{\mathbf{e}}_{\theta,0}$ and arbitrary positive-definite covariance matrix $\bar{\mathbf{\Sigma}}_{\theta,0}$. To demonstrate the effect of the initial choice to the noise parameters estimation, five representative sets of the initial noise parameters are employed. The actual values of the noise parameters are used for Trial 1 while the other four trials represent different combinations of overestimation or underestimation in the initial values. These five sets of

Table 1 Five representative sets of initial noise parameters

Trial	$\bar{e}_{\theta,0}^{(1)}$	$\bar{e}_{\theta,0}^{(2)}$
1	0.0754	1.320×10^{-4}
2	10	10
3	10	10^{-5}
4	10^{-3}	10
5	10^{-3}	10^{-5}

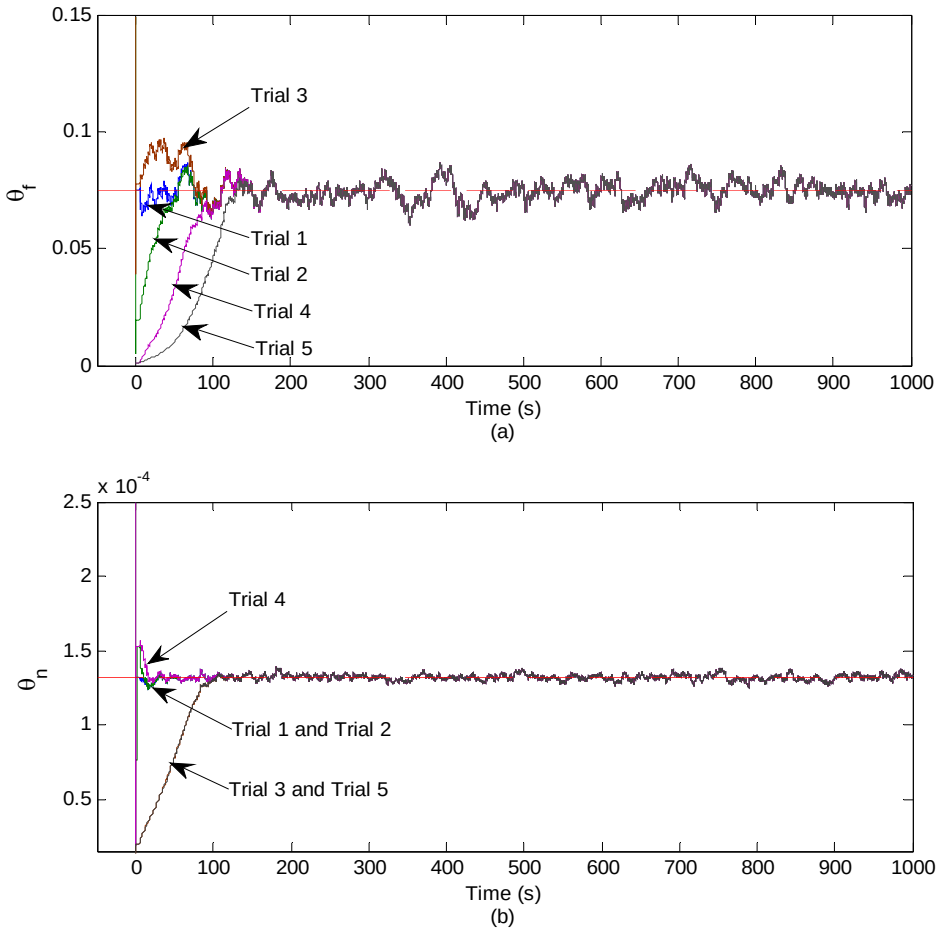

Fig. 1 Estimated noise parameters with different initial conditions (Case 1)

initial values are listed in Table 1. The initial covariance matrix of the noise parameter vector $\bar{\boldsymbol{\Sigma}}_{\theta,0}$ is assigned to be diagonal matrix with large variances: $\bar{\boldsymbol{\Sigma}}_{\theta,0} = 1/9 * \mathrm{diag}\left(\left(\bar{e}_{\theta,0}^{(1)}\right)^2, \left(\bar{e}_{\theta,0}^{(2)}\right)^2\right)$. The rationale for this is to use a prior distribution that covers the actual noise parameters in its

significant region (i.e., within the plus and minus three standard deviations region). Furthermore, this region covers only positive values of the noise parameters by using this prior distribution.

Fig. 1 shows the time histories of the estimated noise parameters for these five trials. The solid lines represent the estimated results of the five trials and the dashed lines represent the actual values. It can be clearly seen that the choice of the initial noise parameters affects only the estimation at the early propagation stage for the proposed approach and all these curves merge to one after the 150th second. It is not surprising that the result with Trial 1 is associated with the fastest convergence for both noise parameters because the actual noise parameters are taken as the initial values. However, the initial noise parameters for other trials are far from the actual values. By comparing the results of Trial 2 to Trial 5, it is found that the trials with larger initial noise parameters are associated with higher convergence rates. For example, Trial 2 converges significantly faster than Trial 3 to Trial 5 and the estimated noise parameters of Trial 1 and Trial 2 become virtually identical since around the 40th second. Taking this into account, an arbitrarily large initial noise parameter vector $\bar{\mathbf{e}}_{\theta,0} = [10, 10]^T$ and the associated initial covariance matrix $\bar{\boldsymbol{\Sigma}}_{\theta,0} = 1/9 * \mathrm{diag}(100, 100)$ (i.e., Trial 2) are used hereafter.

Next, the state estimation performance of the proposed method is compared with the Kalman filter using prescribed noise parameters, namely the actual noise parameters (i.e., $\boldsymbol{\theta} = \widehat{\boldsymbol{\theta}} = [0.0754, 1.320 \times 10^{-4}]^T$) and $\boldsymbol{\theta} = [10, 10]^T$. Note that the parameter vector $\boldsymbol{\theta} = [10, 10]^T$ will

Table 2 RMS errors of the estimated state using the conventional Kalman filter and the proposed method (Case 1)

RMS error	Kalman filter		Proposed method
	$\boldsymbol{\theta} = \widehat{\boldsymbol{\theta}}$	$\boldsymbol{\theta} = [10, 10]^T$	$\bar{\mathbf{e}}_{\theta,0} = [10, 10]^T$
x_5(m)	1.089×10^{-4}	1.051×10^{-3} [865]	1.089×10^{-4} [3.62×10^{-3}]
x_{10}(m)	2.009×10^{-4}	1.869×10^{-3} [830]	2.009×10^{-4} [4.30×10^{-3}]
x_{15}(m)	2.803×10^{-4}	2.531×10^{-3} [803]	2.803×10^{-4} [5.11×10^{-3}]
x_{20}(m)	3.487×10^{-4}	3.076×10^{-3} [782]	3.486×10^{-4} [5.94×10^{-3}]
x_{25}(m)	4.070×10^{-4}	3.525×10^{-3} [766]	4.070×10^{-4} [6.37×10^{-3}]
x_{30}(m)	4.559×10^{-4}	3.889×10^{-3} [753]	4.559×10^{-4} [6.14×10^{-3}]
x_{35}(m)	4.955×10^{-4}	4.176×10^{-3} [743]	4.954×10^{-4} [5.74×10^{-3}]
x_{40}(m)	5.253×10^{-4}	4.389×10^{-3} [736]	5.252×10^{-4} [5.38×10^{-3}]
x_{45}(m)	5.445×10^{-4}	4.524×10^{-3} [731]	5.445×10^{-4} [5.05×10^{-3}]
x_{50}(m)	5.521×10^{-4}	4.576×10^{-3} [729]	5.521×10^{-4} [4.89×10^{-3}]
$\dot{x}_5$(m/s)	9.880×10^{-4}	5.451×10^{-3} [452]	9.882×10^{-4} [1.87×10^{-2}]
$\dot{x}_{10}$(m/s)	1.075×10^{-3}	7.235×10^{-3} [573]	1.076×10^{-3} [1.65×10^{-2}]
$\dot{x}_{15}$(m/s)	1.134×10^{-3}	8.142×10^{-3} [618]	1.134×10^{-3} [1.58×10^{-2}]
$\dot{x}_{20}$(m/s)	1.184×10^{-3}	8.815×10^{-3} [644]	1.184×10^{-3} [1.35×10^{-2}]
$\dot{x}_{25}$(m/s)	1.222×10^{-3}	9.279×10^{-3} [659]	1.222×10^{-3} [1.04×10^{-2}]
$\dot{x}_{30}$(m/s)	1.255×10^{-3}	9.665×10^{-3} [670]	1.255×10^{-3} [8.90×10^{-3}]
$\dot{x}_{35}$(m/s)	1.285×10^{-3}	9.992×10^{-3} [677]	1.285×10^{-3} [8.96×10^{-3}]
$\dot{x}_{40}$(m/s)	1.314×10^{-3}	1.027×10^{-2} [681]	1.315×10^{-3} [9.74×10^{-3}]
$\dot{x}_{45}$(m/s)	1.341×10^{-3}	1.051×10^{-2} [684]	1.341×10^{-3} [1.05×10^{-2}]
$\dot{x}_{50}$(m/s)	1.360×10^{-3}	1.069×10^{-2} [686]	1.361×10^{-3} [1.05×10^{-2}]

Note: The numbers in [ ] denote the percentage of difference.

Table 3 Maximum absolute errors of the estimated state using the conventional Kalman filter and the proposed method (Case 1)

Infinity-norm error	Kalman filter		Proposed method
	$\boldsymbol{\theta} = \widehat{\boldsymbol{\theta}}$	$\boldsymbol{\theta} = [10, 10]^T$	$\bar{\mathbf{e}}_{\theta,0} = [10, 10]^T$
x_5(m)	4.269×10^{-4}	4.151×10^{-3} [872]	4.271×10^{-4} [4.46×10^{-2}]
x_{10}(m)	7.951×10^{-4}	7.180×10^{-3} [803]	7.955×10^{-4} [4.60×10^{-2}]
x_{15}(m)	1.085×10^{-3}	9.206×10^{-3} [749]	1.085×10^{-3} [4.23×10^{-2}]
x_{20}(m)	1.294×10^{-3}	1.095×10^{-2} [746]	1.294×10^{-3} [4.10×10^{-2}]
x_{25}(m)	1.528×10^{-3}	1.253×10^{-2} [720]	1.529×10^{-3} [4.00×10^{-2}]
x_{30}(m)	1.693×10^{-3}	1.349×10^{-2} [697]	1.694×10^{-3} [4.32×10^{-2}]
x_{35}(m)	1.826×10^{-3}	1.417×10^{-2} [676]	1.827×10^{-3} [1.41×10^{-2}]
x_{40}(m)	1.941×10^{-3}	1.482×10^{-2} [664]	1.940×10^{-3} [1.26×10^{-2}]
x_{45}(m)	2.043×10^{-3}	1.551×10^{-2} [659]	2.043×10^{-3} [8.42×10^{-3}]
x_{50}(m)	2.087×10^{-3}	1.584×10^{-2} [659]	2.087×10^{-3} [6.13×10^{-3}]
$\dot{x}_5$(m/s)	4.393×10^{-3}	2.664×10^{-2} [506]	4.370×10^{-3} [5.32×10^{-1}]
$\dot{x}_{10}$(m/s)	4.721×10^{-3}	3.777×10^{-2} [700]	4.736×10^{-3} [2.98×10^{-1}]
$\dot{x}_{15}$(m/s)	4.962×10^{-3}	4.219×10^{-2} [750]	4.976×10^{-3} [2.74×10^{-1}]
$\dot{x}_{20}$(m/s)	5.005×10^{-3}	4.211×10^{-2} [741]	5.006×10^{-3} [2.71×10^{-2}]
$\dot{x}_{25}$(m/s)	5.245×10^{-3}	4.380×10^{-2} [735]	5.245×10^{-3} [2.98×10^{-3}]
$\dot{x}_{30}$(m/s)	5.282×10^{-3}	4.459×10^{-2} [744]	5.282×10^{-3} [1.58×10^{-2}]
$\dot{x}_{35}$(m/s)	5.311×10^{-3}	4.264×10^{-2} [703]	5.339×10^{-3} [5.11×10^{-1}]
$\dot{x}_{40}$(m/s)	5.724×10^{-3}	4.401×10^{-2} [669]	5.757×10^{-3} [5.71×10^{-1}]
$\dot{x}_{45}$(m/s)	5.924×10^{-3}	4.304×10^{-2} [627]	5.958×10^{-3} [5.65×10^{-1}]
$\dot{x}_{50}$(m/s)	5.928×10^{-3}	4.495×10^{-2} [658]	5.962×10^{-3} [5.69×10^{-1}]

Note: The numbers in [ ] denote the percentage of difference.

also be used as the initial values for the proposed method. The accuracy of state estimation is evaluated according to the RMS errors and the maximum absolute errors of the estimated state variables. These results are summarized in Tables 2 and 3, respectively. In order to eliminate the effect of the initial conditions, the results of the first 100s are excluded from the calculation of the RMS errors and the maximum absolute errors. For the proposed method and the Kalman filter with $\boldsymbol{\theta} = [10, 10]^T$, the numbers in brackets denote the percentage of difference compared with the results of the Kalman filter using the actual noise parameters. Table 2 confirms that the proposed method can achieve satisfactory accuracy of state estimation. Specifically, it demonstrates that the RMS errors of the proposed method with the initial parameters $\bar{\mathbf{e}}_{\theta,0} = [10, 10]^T$ are virtually identical to those of the Kalman filter with the actual noise parameters. The corresponding percentage of difference is less than 0.02% for all state variables. However, the accuracy of state estimation of the conventional Kalman filter is seriously degraded by the inappropriate choice of the noise parameters. By using $\boldsymbol{\theta} = [10, 10]^T$ for the conventional Kalman filter, the RMS errors of the estimated state variables are around one order larger than those obtained with the actual noise parameters. Note that the same results are obtained by using $\boldsymbol{\theta} = [\sigma^2, \sigma^2]^T$, e.g, $\boldsymbol{\theta} = [0.1, 0.1]^T$. On the other hand, the maximum absolute errors are used as an alternative measure of the estimation accuracy. Table 3 reconfirms, in terms of maximum absolute errors, the observation from Table 2. Specifically, the state estimation accuracy of the Kalman filter depends on the

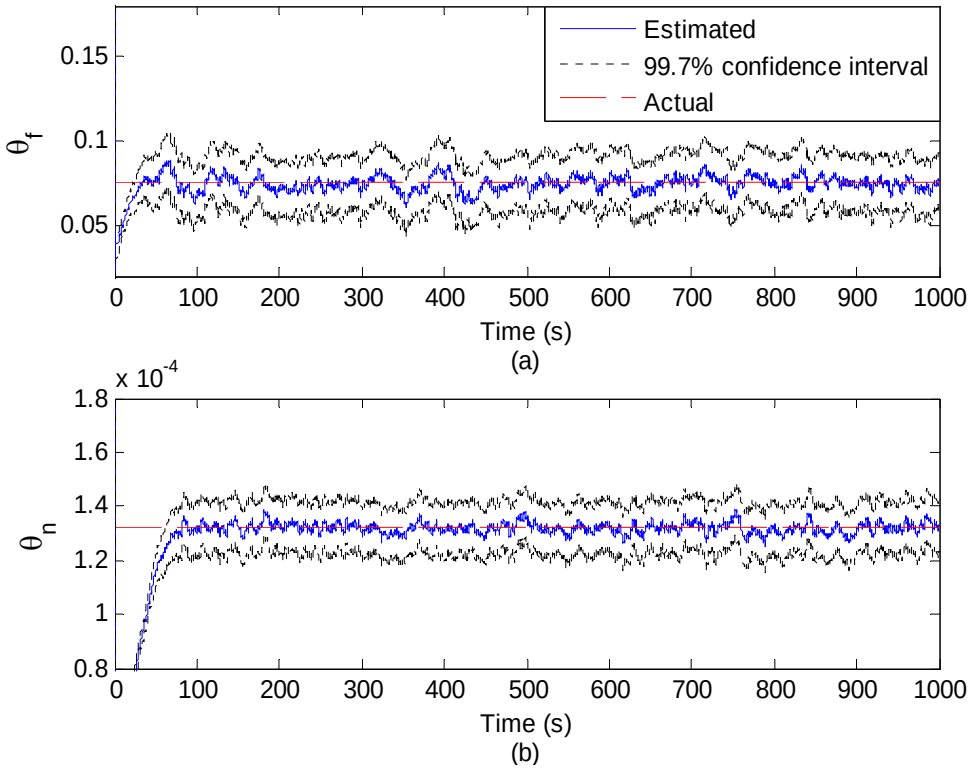

Fig. 2 Estimation results of the noise parameters (Case 1)

choice of the noise parameters. Nevertheless, the proposed method provides accurate state estimation regardless of the poor initial choice of the noise parameters.

Finally, the tracking performance of noise parameters using the proposed method is discussed. Since both the excitation and measurement noise are stationary in this case, the actual noise parameters remain constant throughout the entire monitoring duration. Fig. 2 shows the estimation results of the noise parameters. The solid lines represent the estimated values, the dotted lines represent the plus and minus three standard derivations confidence intervals (i.e., corresponding to a probability of 99.7%) and the dashed lines represent the actual values of the noise parameters. For both of the noise parameters, the estimated results approach to the actual values after 70s with reasonable confidence intervals. This example demonstrates that reliable estimation of the noise parameters is necessary in order to ensure the accuracy of the state estimation. The proposed method provides an efficient solution for this task. In contrast to the conventional usage of Kalman filter, the proposed method requires only a set of arbitrarily positive initial noise parameters. Furthermore, this example verifies that the arbitrary choice of the initial noise parameters does not affect the accuracy of the proposed method after the training process. In practice, it is suggested to start with sufficiently large initial values of the noise parameters.

Table 4 RMS errors of the estimated state using the conventional Kalman filter and the proposed method (Case 2)

RMS error	Kalman filter				Proposed method
	$\boldsymbol{\theta}=\widehat{\boldsymbol{\theta}}$	$\boldsymbol{\theta}=\bar{\widehat{\boldsymbol{\theta}}}$	$\boldsymbol{\theta}=\widehat{\boldsymbol{\theta}}_0$	$\boldsymbol{\theta}=[10,10]^T$	$\bar{\mathbf{e}}_{\theta,0}=[10,10]^T$
$x_5(\mathrm{m})$	1.397×10^{-4}	1.397×10^{-4}	1.397×10^{-4}	9.956×10^{-4}	1.397×10^{-4}
$x_{10}(\mathrm{m})$	2.576×10^{-4}	2.576×10^{-4}	2.576×10^{-4}	1.764×10^{-3}	2.576×10^{-4}
$x_{15}(\mathrm{m})$	3.594×10^{-4}	3.593×10^{-4}	3.593×10^{-4}	2.383×10^{-3}	3.593×10^{-4}
$x_{20}(\mathrm{m})$	4.471×10^{-4}	4.470×10^{-4}	4.469×10^{-4}	2.893×10^{-3}	4.470×10^{-4}
$x_{25}(\mathrm{m})$	5.219×10^{-4}	5.218×10^{-4}	5.217×10^{-4}	3.312×10^{-3}	5.218×10^{-4}
$x_{30}(\mathrm{m})$	5.846×10^{-4}	5.845×10^{-4}	5.844×10^{-4}	3.653×10^{-3}	5.846×10^{-4}
$x_{35}(\mathrm{m})$	6.353×10^{-4}	6.351×10^{-4}	6.350×10^{-4}	3.922×10^{-3}	6.352×10^{-4}
$x_{40}(\mathrm{m})$	6.735×10^{-4}	6.733×10^{-4}	6.732×10^{-4}	4.121×10^{-3}	6.734×10^{-4}
$x_{45}(\mathrm{m})$	6.982×10^{-4}	6.981×10^{-4}	6.979×10^{-4}	4.248×10^{-3}	6.981×10^{-4}
$x_{50}(\mathrm{m})$	7.079×10^{-4}	7.078×10^{-4}	7.076×10^{-4}	4.297×10^{-3}	7.079×10^{-4}
$\dot{x}_5(\mathrm{m/s})$	1.232×10^{-3}	1.263×10^{-3}	1.284×10^{-3}	5.639×10^{-3}	1.235×10^{-3}
$\dot{x}_{10}(\mathrm{m/s})$	1.347×10^{-3}	1.376×10^{-3}	1.394×10^{-3}	7.261×10^{-3}	1.349×10^{-3}
$\dot{x}_{15}(\mathrm{m/s})$	1.423×10^{-3}	1.451×10^{-3}	1.468×10^{-3}	8.073×10^{-3}	1.426×10^{-3}
$\dot{x}_{20}(\mathrm{m/s})$	1.489×10^{-3}	1.516×10^{-3}	1.532×10^{-3}	8.680×10^{-3}	1.491×10^{-3}
$\dot{x}_{25}(\mathrm{m/s})$	1.539×10^{-3}	1.564×10^{-3}	1.580×10^{-3}	9.097×10^{-3}	1.541×10^{-3}
$\dot{x}_{30}(\mathrm{m/s})$	1.582×10^{-3}	1.606×10^{-3}	1.622×10^{-3}	9.446×10^{-3}	1.584×10^{-3}
$\dot{x}_{35}(\mathrm{m/s})$	1.621×10^{-3}	1.645×10^{-3}	1.660×10^{-3}	9.744×10^{-3}	1.623×10^{-3}
$\dot{x}_{40}(\mathrm{m/s})$	1.659×10^{-3}	1.682×10^{-3}	1.697×10^{-3}	9.999×10^{-3}	1.661×10^{-3}
$\dot{x}_{45}(\mathrm{m/s})$	1.694×10^{-3}	1.716×10^{-3}	1.731×10^{-3}	1.022×10^{-2}	1.696×10^{-3}
$\dot{x}_{50}(\mathrm{m/s})$	1.719×10^{-3}	1.741×10^{-3}	1.756×10^{-3}	1.038×10^{-2}	1.721×10^{-3}

4.2 Case 2: Nonstationary ground excitation with stationary measurement noise

In this case, the underlying shear building is subjected to nonstationary ground excitation. The force distributing matrix is given by $\mathbf{T}_0=\mathbf{M}[-1,-1,\ldots,-1]^T$ and the nonstationary ground excitation is modeled as a modulated zero-mean Gaussian white noise $\mathbf{f}(t)=\mathbf{F}(t)=\ddot{g}(t)=A_f(t)v(t)$, where v is a stationary Gaussian white noise with spectral intensity $S_{v0}=1.20\times10^{-4}\mathrm{m}^2/\mathrm{s}^3$. The modulating function A_f is given by

$$A_f(t)=\begin{cases}1+0.2\sin(2\pi t/50), & 0\le t<300\mathrm{s}\\ 1+4(t-300)\exp[-0.02(t-100)], & 300\mathrm{s}\le t<700\mathrm{s}\\ 1-0.2\sin(2\pi t/50), & 700\mathrm{s}\le t\le1000\mathrm{s}\end{cases} \tag{28}$$

The measurement noise is modeled as stationary Gaussian white noise. The RMS of the measurement noise is taken to be 5% RMS of the noise-free acceleration of the top floor so that the covariance matrix of the measurement noise can be expressed as $\boldsymbol{\Sigma}_{n,k+1}=\sigma_{n,k+1}^2\mathbf{I}$. Again, the noise parameter vector is taken to be $\boldsymbol{\theta}_{k+1}=\left[\theta_{f,k},\theta_{n,k+1}\right]^T$ where $\theta_{f,k}=\sigma_{f,k}^2$ and $\theta_{n,k+1}=\sigma_{n,k+1}^2$.

Table 4 shows the RMS errors of the estimated state obtained by the Kalman filter with

prescribed noise parameters and the proposed method with the initial parameters $\bar{\mathbf{e}}_{\theta,0} = [10, 10]^T$. For the Kalman filter, four trials of noise parameters are used: the actual time-varying noise parameters, i.e., $\boldsymbol{\theta} = \widehat{\boldsymbol{\theta}}$; the mean values of the actual noise parameters, i.e., $\boldsymbol{\theta} = \overline{\widehat{\boldsymbol{\theta}}}$; the actual noise parameters at $t = 0$, i.e., $\boldsymbol{\theta} = \widehat{\boldsymbol{\theta}}_0$; and the initial noise parameters employed in the proposed approach, i.e., $\boldsymbol{\theta} = [10, 10]^T$. Again, the state estimation results of the first 100s are excluded from the calculation of the RMS errors so that the effect of the initial conditions can be eliminated.

These results show that the proposed approach is able to provide accurate state estimation and the obtained RMS errors are virtually the same as those of the Kalman filter with the actual time-varying noise parameters. Then, the performance of the conventional Kalman filter with the prescribed noise parameters (i.e., $\boldsymbol{\theta} = \overline{\widehat{\boldsymbol{\theta}}}$, $\boldsymbol{\theta} = \widehat{\boldsymbol{\theta}}_0$ and $\boldsymbol{\theta} = [10, 10]^T$) is discussed. By taking either the mean or the initial values of the actual noise parameters, the utilized noise parameters are close to the actual noise parameters. It turns out that the estimated displacements are fairly accurate with similar RMS errors with the results obtained from the Kalman filter with the actual time-varying noise parameters. However, the RMS errors of the estimated velocity are up to 2.5% of difference for $\boldsymbol{\theta} = \overline{\widehat{\boldsymbol{\theta}}}$ and up to 4% for $\boldsymbol{\theta} = \widehat{\boldsymbol{\theta}}_0$. It is realized that the accuracy of the state estimation is deteriorated even though the prescribed noise parameters are very close to the actual values of the noise parameters. Moreover, it should be noted that these accurate prescribed values of the noise parameters are difficult to achieve in practice. Arbitrarily selected noise parameters induce notable errors on the state estimation. Herein, the RMS errors of the state estimation obtained by the arbitrary selected noise parameters $\boldsymbol{\theta} = [10, 10]^T$ are more than four times larger than the corresponding results obtained by the proposed approach. From this case, it demonstrates the necessity of reliable online estimation on the time-varying noise parameters and the efficacy of the proposed approach to tackle this problem.

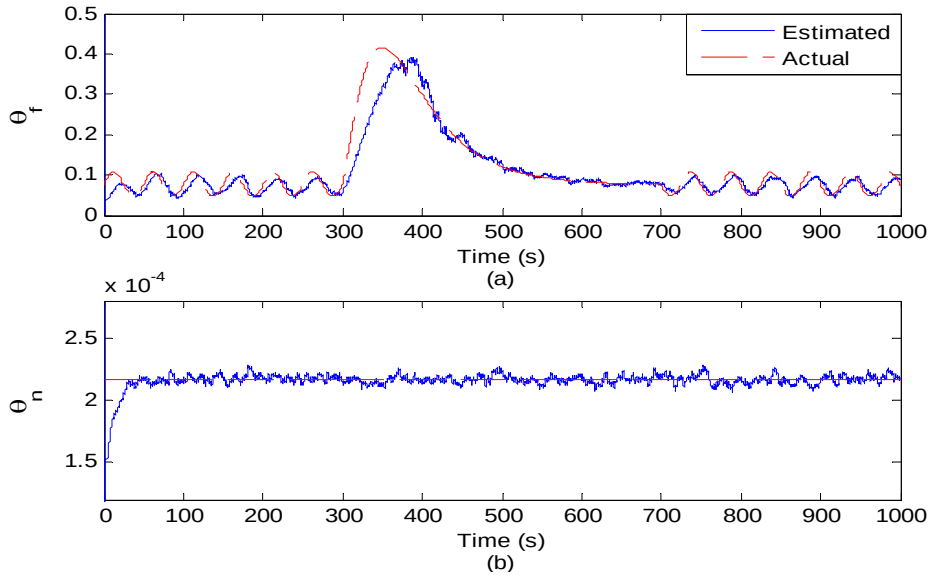

Fig. 3 Comparison between the estimated and actual values of the noise parameters (Case 2)

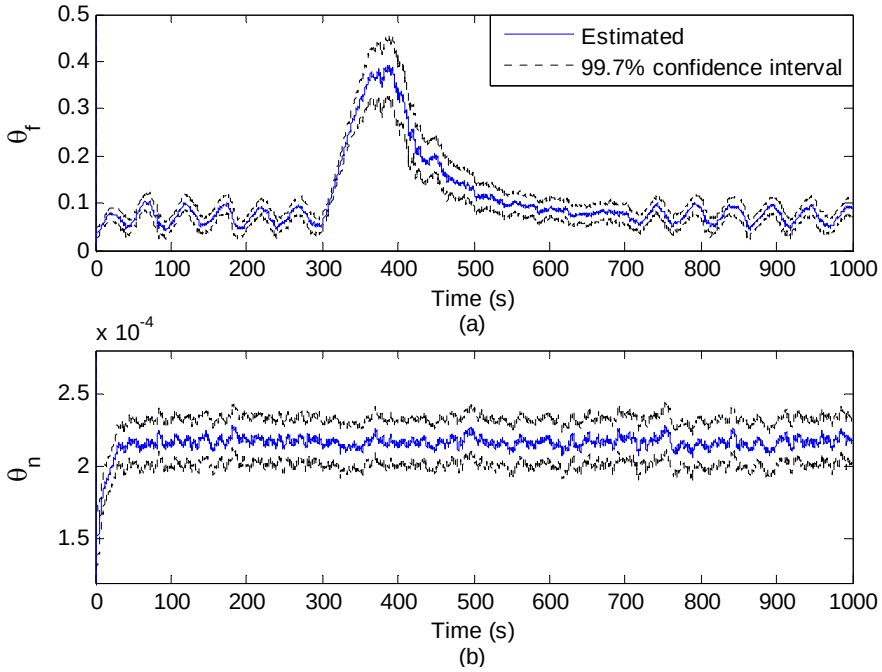

Fig. 4 Estimated noise parameters with 99.7% confidence intervals (Case 2)

Fig. 3 shows the comparison between the estimated and actual noise parameters. Although the fluctuation of the earthquake ground motion is severe, the proposed method performs satisfactorily in tracking the variation. It is observed that there is time delay of the estimated noise parameters. This time lag is expected because the estimation is based on the data at the current and previous time steps. Therefore, the estimation can be viewed as a weighted average of the actual values in a moving time window. Fig. 4 shows the time histories of the estimated noise parameters with the 99.7% confidence intervals. These results confirm that the proposed method provides satisfactory estimation on the noise parameters with reasonable confidence intervals. Through this case, the proposed method is confirmed to be applicable for nonstationary process noise with stationary measurement noise. On the other hand, the conventional Kalman filter cannot achieve accurate state estimation in this situation unless the entire time histories of the covariance matrices of the process noise and measurement noise are given. Unfortunately, this is rarely the case in practice.

4.3 Case 3: Nonstationary wind excitation with nonstationary measurement noise

In the last case, the proposed method is demonstrated with an application under nonstationary process noise and nonstationary measurement noise. Here, the building is subjected to nonstationary wind excitation which is a superposition of the mean wind load $\mathbf{F}_D$ and the turbulent wind load $\mathbf{F}$, i.e., $\mathbf{f}(t) = \mathbf{F}_D + \mathbf{F}(t)$ (Simiu and Scanlan 1996, Taranath 2005). The mean wind load is denoted as $\mathbf{F}_D = \left[\mathrm{F}_D(h_1), \mathrm{F}_D(h_2), \ldots, \mathrm{F}_D\left(h_{N_d}\right)\right]^T$, where h_i is the elevation of the ith floor. The component corresponding to the ith floor $\mathrm{F}_D(h_i)$ is given by

Table 5 RMS errors of the estimated state using the conventional Kalman filter and the proposed method (Case 3)

RMS error	Kalman filter		Proposed method
	$\boldsymbol{\theta}=\widehat{\boldsymbol{\theta}}$	$\boldsymbol{\theta}=[10,10]^T$	$\bar{\mathbf{e}}_{\theta,0}=[10,10]^T$
$x_5(\mathrm{m})$	8.309×10^{-5}	6.240×10^{-4}	8.304×10^{-5}
$x_{10}(\mathrm{m})$	1.607×10^{-4}	1.197×10^{-3}	1.606×10^{-4}
$x_{15}(\mathrm{m})$	2.348×10^{-4}	1.714×10^{-3}	2.346×10^{-4}
$x_{20}(\mathrm{m})$	3.006×10^{-4}	2.179×10^{-3}	3.004×10^{-4}
$x_{25}(\mathrm{m})$	3.638×10^{-4}	2.590×10^{-3}	3.635×10^{-4}
$x_{30}(\mathrm{m})$	4.170×10^{-4}	2.946×10^{-3}	4.166×10^{-4}
$x_{35}(\mathrm{m})$	4.667×10^{-4}	3.244×10^{-3}	4.662×10^{-4}
$x_{40}(\mathrm{m})$	5.039×10^{-4}	3.478×10^{-3}	5.033×10^{-4}
$x_{45}(\mathrm{m})$	5.356×10^{-4}	3.635×10^{-3}	5.351×10^{-4}
$x_{50}(\mathrm{m})$	5.464×10^{-4}	3.699×10^{-3}	5.459×10^{-4}
$\dot{x}_5(\mathrm{m/s})$	2.776×10^{-4}	1.617×10^{-3}	2.776×10^{-4}
$\dot{x}_{10}(\mathrm{m/s})$	4.026×10^{-4}	2.405×10^{-3}	4.026×10^{-4}
$\dot{x}_{15}(\mathrm{m/s})$	5.484×10^{-4}	2.901×10^{-3}	5.483×10^{-4}
$\dot{x}_{20}(\mathrm{m/s})$	6.282×10^{-4}	3.289×10^{-3}	6.282×10^{-4}
$\dot{x}_{25}(\mathrm{m/s})$	7.499×10^{-4}	3.625×10^{-3}	7.498×10^{-4}
$\dot{x}_{30}(\mathrm{m/s})$	7.955×10^{-4}	3.928×10^{-3}	7.953×10^{-4}
$\dot{x}_{35}(\mathrm{m/s})$	9.030×10^{-4}	4.228×10^{-3}	9.026×10^{-4}
$\dot{x}_{40}(\mathrm{m/s})$	9.364×10^{-4}	4.536×10^{-3}	9.359×10^{-4}
$\dot{x}_{45}(\mathrm{m/s})$	1.017×10^{-3}	4.869×10^{-3}	1.016×10^{-3}
$\dot{x}_{50}(\mathrm{m/s})$	1.138×10^{-3}	5.173×10^{-3}	1.138×10^{-3}

$$\mathrm{F}_D(h_i)=\frac{1}{2}\,\rho\,\widetilde{U}_H^2\,c_D\,A_w(h_i/H)^{2\beta} \tag{29}$$

where the air density is $\rho=1.20\mathrm{kg/m^3}$; the reference height is $H=10\mathrm{m}$; the mean wind velocity at the reference height H is $\widetilde{U}_H=10\mathrm{m/s}$; the drag coefficient is $c_D=2.03$; the equivalent windward area of one story is $A_w=20\times2.5=50\mathrm{m^2}$; and the power-law exponent is $\beta=0.3$. The turbulent wind load $\mathbf{F}(t)=A_f(t)\mathbf{g}(t)$ is modeled as a modulated zero-mean Gaussian white noise. The modulating function A_f is given by:

$$A_f(t)=\begin{cases}1+t/500, & 0\le t<500\mathrm{s}\\ 3-t/500, & 500\mathrm{s}\le t\le 1000\mathrm{s}\end{cases} \tag{30}$$

The (i,j) component of the covariance matrix $\mathbf{\Sigma}_g^0$ of $\mathbf{g}(t)$ can be expressed as:

$$\mathbf{\Sigma}_g^{0(i,j)}=\gamma^2 r^{(i,j)}\mathrm{F}_D(h_i)\mathrm{F}_D(h_j),\qquad i,j=1,\dots,N_d \tag{31}$$

where $\gamma=0.2$ is the intensity of the turbulence wind at the reference height H; and the correlation coefficient between h_i and h_j is expressed as $r^{(i,j)}=\exp\left(-\left|h_i-h_j\right|/H\right)$. In this case, the force distributing matrix is $\mathbf{T}_0=\mathbf{I}$. Therefore, the covariance matrix of the excitation can be expressed as $\mathbf{\Sigma}_{f,k}=\sigma_{f,k}^2\mathbf{\Sigma}_g^0$. On the other hand, the measurement noise is modeled as

modulated stationary Gaussian white noise. For simulation purpose, the same modulating function is employed but this information is assumed unavailable in the identification process. The RMS of the stationary Gaussian white noise is taken to be 5% RMS of the noise-free acceleration of the top floor.

The RMS errors of the estimated state variables are used to evaluate the accuracy of state estimation. Table 5 shows the comparison between the RMS errors of the estimated state using the proposed method and the Kalman filter. In particular, the results obtained by the proposed method is compared with those obtained by the Kalman filter with the actual time-varying noise parameter $\boldsymbol{\theta} = \widehat{\boldsymbol{\theta}}$ and the initial noise parameters employed in the proposed approach $\boldsymbol{\theta} = [10, 10]^T$. Again, the results of the first 100s are excluded from the calculation of the RMS errors so that the effect of the initial conditions can be eliminated. Since the RMS errors obtained from the proposed approach are virtually identical to those of the Kalman filter with the actual noise parameters, it reconfirms that the proposed approach provides accurate state estimation. Besides, it is clearly seen that the RMS errors of the proposed method are much lower than those of the conventional Kalman filter. The accuracy of the conventional Kalman filter with $\boldsymbol{\theta} = [10, 10]^T$ is poor. By using the proposed method, the accuracy of state estimation is significantly improved.

Fig. 5 shows the time histories of the estimated and actual noise parameters. It is observed that the variations for both noise parameters can be successfully estimated. In addition, the time histories of the estimated noise parameters with the 99.7% confidence intervals are shown in Fig. 6. It is realized that the proposed method can track the time-varying noise parameters and provide the confidence intervals of the estimation. These results verify that the proposed method is

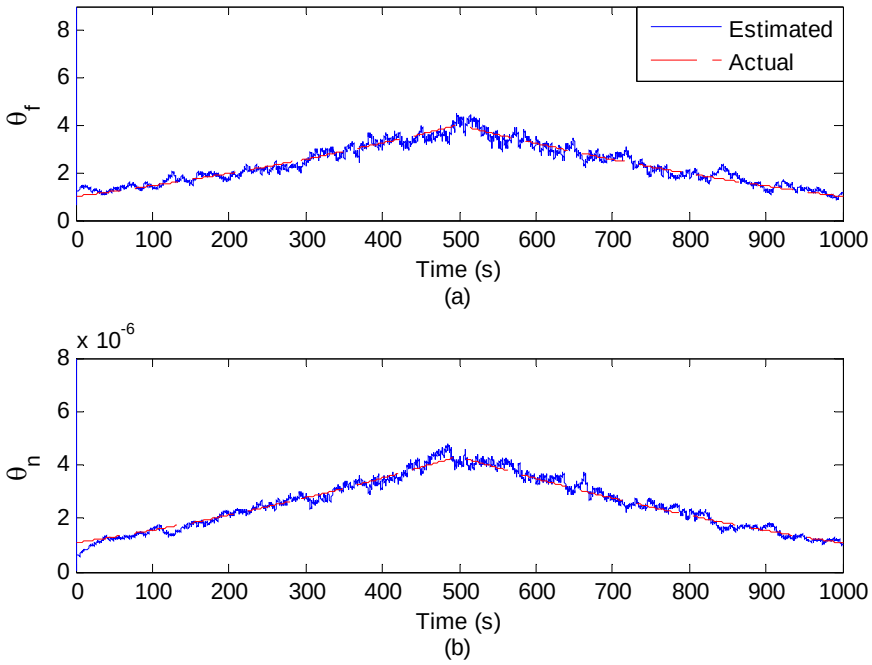

Fig. 5 Comparison between the estimated and actual values of the noise parameters (Case 3)

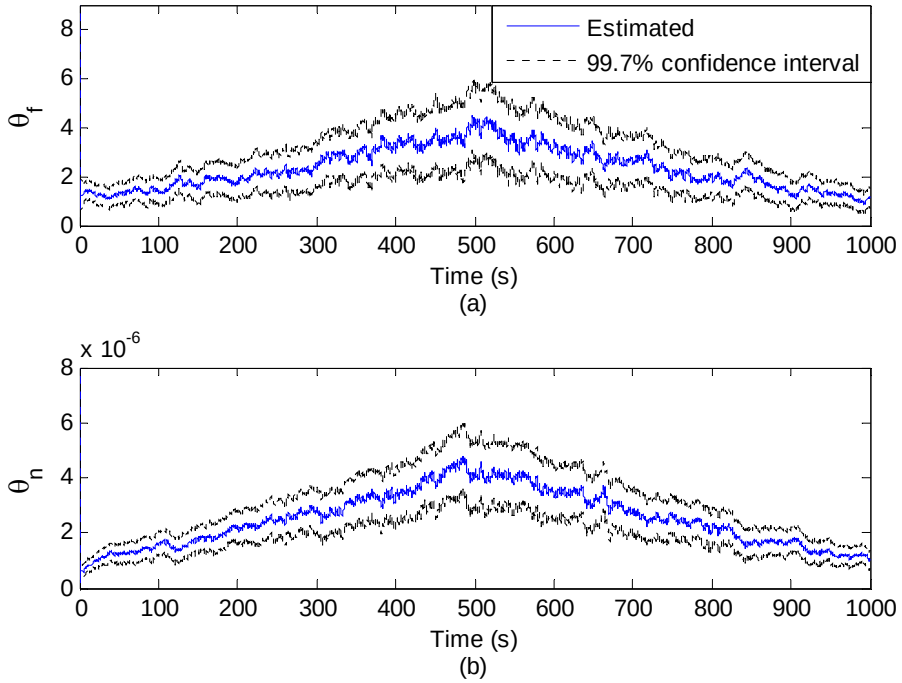

Fig. 6 Estimated noise parameters with 99.7% confidence intervals (Case 3)

capable for general situations with nonstationary process noise and nonstationary measurement noise. The estimated noise parameters are accurate and the associated estimation uncertainties are reliable. Consequently, reliable state estimation can be achieved.

5. Conclusions

The noise covariance matrices are required for state estimation using the Kalman filter. However, prior information of these noise covariance matrices is usually not available in practice and inappropriate choice substantially deteriorates the accuracy of state estimation results. In this study, a Bayesian probabilistic method is proposed for online estimation of the noise parameters which govern the noise covariance matrices. The proposed method is a two-stage approach that includes a training stage before the operating stage. The training stage is necessary because the initial noise parameters may be far from the actual values. Direct application of the gradient-type of methods leads to erroneous results. Moreover, the proposed method removes the stationarity requirement imposed to the process noise and measurement noise. Therefore, it is widely applicable for state estimation in nonstationary situation. The efficacy and efficiency of the proposed method were confirmed by the illustrative examples. Three stationarity scenarios of the process noise and measurement noise were examined. These results confirm that the proposed method successfully provides reliable online estimation of the noise parameters for both stationary and nonstationary situations. Consequently, accurate online state estimation can be accomplished by using the proposed method.

Acknowledgments

This work was supported by the Research Committee of University of Macau under Research Grant RG059/09-10S/11R/YKV/FST and the Science and Technology Development Fund (FDCT) of the Macau government under Research Grant 012/2013/A1. These generous supports are gratefully acknowledged.

References

Beck, J.L. (2010), "Bayesian system identification based on probability logic", *Struct. Control Hlth.*, **17**(7), 825-847.

Beck, J.L. and Katafygiotis, L.S. (1998), "Updating models and their uncertainties, I: Bayesian statistical framework", *J. Eng. Mech.-ASCE*, **124**(4), 455-461.

Beck, J.L. and Yuen, K.V. (2004), "Model selection using response measurements: Bayesian probabilistic approach", *J. Eng. Mech.-ASCE*, **130**(2), 192-203.

Box, G.E.P. and Tiao, G.C. (1973), *Bayesian Inference in Statistical Analysis*, Addison-Wesley, Reading, MA.

Ching, J., Beck, J.L. and Porter, K.A. (2006), "Bayesian state and parameter estimation of uncertain dynamical systems", *Probabilist. Eng. Mech.*, **21**(1), 81-96.

Ching, J., Porter, K.A. and Beck, J.L. (2009), "Propagating uncertainties for loss estimation in performance-based earthquake engineering using moment matching", *Struct. Infrastruct. E.*, **5**(3), 245-262.

Chui, C.K. and Chen, G. (2009), *Kalman Filtering with Real-Time Applications*, 4th Edition, Springer-Verlag, New York.

Grewal, M.S. and Andrews, A.P. (1993), *Kalman Filtering: Theory and Practice*, Prentice Hall, Englewood Cliffs, New Jersey.

Hoi, K.I., Yuen, K.V. and Mok, K.M. (2008), "Kalman filter based prediction system for wintertime PM10 concentrations in Macau", *Global NEST J.*, **10**(2), 140-150.

Kalman, R.E. (1960), "A new approach to linear filtering and prediction problems", *J. Basic Eng.-T. ASME*, **82**(1), 35-45.

Koh, C.G. and See, L.M. (1994), "Identification and uncertainty estimation of structural parameters", *J. Eng. Mech.-ASCE*, **120**(6), 1219-1236.

Kuok, S.C. and Yuen, K.V. (2012), "Structural health monitoring of Canton tower using Bayesian framework", *Smart Struct. Syst.*, **10**(4-5), 375-391.

Lam, H.F., Yuen, K.V. and Beck, J.L. (2006), "Structural health monitoring via measured Ritz vectors utilizing artificial neural networks", *Comput. Aided Civ. Inf.*, **21**(4), 232-241.

Lee, M.H. and Chen, T.C. (2010), "Intelligent fuzzy weighted input estimation method for the input force on the plate structure", *Struct. Eng. Mech.*, **34**(1), 1-14.

Lei, Y. and Jiang, Y.Q. (2011), "A two-stage Kalman estimation approach for the identification of structural parameters under unknown inputs", *Adv. Mat. Res.*, **243-249**, 5394-5398.

Lin, J.W., Chen, C.W. and Hsu, T.C. (2013), "A novel regression prediction model for structural engineering applications", *Struct. Eng. Mech.*, **45**(5), 693-702.

Mehra, R.K. (1970), "On the identification of variance and adaptive Kalman filtering", *IEEE T. Automat. Contr.*, **15**(2), 175-184.

Mohamed, A.H. and Schwarz, K.P. (1999), "Adaptive Kalman filtering for INS/GPS", *J. Geodesy*, **73**, 193-203.

Ni, Y.Q., Ko, J.M., Hua, X.G. and Zhou, H.F. (2007), "Variability of measured modal frequencies of a cable-stayed bridge under different wind conditions", *Smart Struct. Syst.*, **3**(3), 341-356.

Odelson, B.J., Rajamani, M.R. and Rawlings, J.B. (2006), "A new autocovariance least-squares method for

estimating noise covariances", *Automatica*, **42**(2), 303-308.
Papadimitriou, C., Beck, J.L. and Au, S.K. (2000), "Entropy-based optimal sensor location for structural model updating", *J. Vib. Control*, **6**(5), 781-800.
Papadimitriou, C., Fritzen, C.P., Kraemer, P. and Ntotsios, E. (2011), "Fatigue predictions in entire body of metallic structures from a limited number of vibration sensors using Kalman filtering", *Struct. Control Hlth.*, **18**(5), 554-573.
Rosa, L., Tomasini, G., Zasso, A. and Aly, A.M. (2012), "Wind-induced dynamics and loads in a prismatic slender building: modal approach based on unsteady pressure measures", *J. Wind Eng. Ind. Aerod.*, **107-108**, 118-130.
Sangsuk-Iam, S. and Bullock, T.E. (1990), "Analysis of discrete time Kalman filtering under incorrect noise covariances", *IEEE T. Automat. Contr.*, **35**(12), 1304-1309.
Schmidt, S.F. (1981), "The Kalman filter: Its recognition and development for aerospace applications", *J. Guid. Control Dynam.*, **4**(1), 4-7.
Simiu, E. and Scanlan, R.H. (1996), *Wind Effects on Structures, Fundamentals and Applications to Design*, 3rd Edition, John Wiley & Sons.
Sorensen, S.W. and Sacks, J.E. (1971), "Recursive fading memory filters", *Inform. Sciences*, **3**(2), 101-119.
Taranath, B.S. (2005), *Wind and Earthquake Resistant Buildings: Structural Analysis and Design*, New York, Marcel Dekker.
Yan, W.M., Yuen, K.V. and Yoon, G.L. (2009), "Bayesian probabilistic approach for correlations of compressibility index for marine clays", *J. Geotech. Geoenviron.*, **135**(12), 1932-1940.
Yang, J.N., Lei, Y., Lin, S. and Huang, N. (2004), "Identification of natural frequencies and dampings of in situ tall buildings using ambient wind vibration data", *J. Eng. Mech.-ASCE*, **130**(5), 570-577.
Yuen, K.V. (2010), *Bayesian Methods for Structural Dynamics and Civil Engineering*, John Wiley and Sons, New York.
Yuen, K.V., Hoi, K.I. and Mok, K.M. (2007), "Selection of noise parameters for Kalman filter", *Earthq. Eng. Eng. Vib.*, **6**(1), 49-56.
Yuen, K.V. and Katafygiotis, L.S. (2001), "Bayesian time-domain approach for modal updating using ambient data", *Probabilist. Eng. Mech.*, **16**(3), 219-231.
Yuen, K.V. and Katafygiotis, L.S. (2005a), "An efficient simulation method for reliability analysis using simple additive rules of probability", *Probabilist. Eng. Mech.*, **20**(1), 109-114.
Yuen, K.V. and Katafygiotis, L.S. (2005b), "Model updating using noisy response measurements without knowledge of the input spectrum", *Earthq. Eng. Struct. Dyn.*, **34**(2), 167-187.
Yuen, K.V. and Kuok, S.C. (2010), "Ambient interference in long-term monitoring of buildings", *Eng. Struct.*, **32**(8), 2379-2386.
Yuen, K.V. and Kuok, S.C. (2011), "Bayesian methods for updating dynamic models", *Appl. Mech. Rev.*, **64**(1), 010802-1-010802-18.
Yuen, K.V. and Mu, H.Q. (2012), "A novel probabilistic method for robust parametric identification and outlier detection", *Probabilist. Eng. Mech.*, **30**, 48-59.
Yun, C.B., Abdelrahman, A.M. and Wang, P.C. (1979), "Along-wind gust effect on elevated structures", *Eng. Struct.*, **1**(3), 121-124.